Technical Memorandum

To: Jeff Uhlmeyer

From: Gary Elkins, Pedro Serigos, Lauren Gardner, Gonzalo Rada and Kevin Senn

cc: Mustafa Mohamedali

Date: April 3, 2020 (original)

Re. Forensic Desktop Study Report: Florida SPS-5 Project

The Long-Term Pavement Performance (LTPP) Specific Pavement Studies (SPS) test sections 12_0502, 12_0503, 12_0504, 12_0505, 12_0506, 12_0507, 12_0508, 12_0509, 12_0561, 12_0562, 12_0563, 12_0564, 12_0565, and 12_0566[1] and General Pavement Studies (GPS) control test section 12_1030[2] were nominated for a desktop study under TPF-5(332) "LTPP Forensic Evaluations." The LTPP SPS-5 experiment is a study of asphalt concrete (AC) overlay on AC pavements.

Table 1 shows the main experimental features of the test sections at this site. The pavement treatment factors included in the main LTPP SPS-5 experimental design consisted of the control section and eight test sections with varying intensity of surface preparation before the overlay, the type of material used for overlay (recycled asphalt concrete (RAP) versus virgin AC mixtures), and nominal overlay thickness (2 or 5 inches). Another six supplemental test sections at the site were designed by the Florida Department of Transportation (DOT) with virgin AC and RAP mixes, an overlay and two mill and inlay sections of varying thickness. The control section is considered the do-nothing regular maintenance test section and is intended to track deterioration of the pavement structure without overlay.

The test sections at the Florida SPS-5 site have a wet – no freeze climate classification, are located on coarse grained soil, and were judged to be in poor condition at the time of overlay. Since the test sections at each SPS-5 site are subjected to the same climate, have similar subgrade soils and traffic loading conditions, and a relatively uniform pavement structure on all sections prior to overlay, the experimental factors that are the focus of this desktop study are overlay mix type, surface conditions prior to overlay, surface preparation and overlay thickness.

[1] First two digits in test section number represent the State Code [12= Florida]. For LTPP GPS test sections, the final four digits are unique within each State/Province and were assigned at the time the test section was accepted into the LTPP program. For LTPP Specific Pavement Studies (SPS) test sections, the second set of two numbers indicates the Project Code (e.g., 05 = SPS-5), and the final set of two numbers represents the test section number on that project (e.g., 04).

[2] Note that section 12_1030 does not have a SPS- 5 related SHRP_ID because it was an existing LTPP GPS test section prior to construction of the SPS-5 test sections. It serves as the "do-nothing" or normal maintenance control section where an overlay layer was not placed at the time the overlay on the other test sections at this site were constructed.

The purpose of this forensic study was to investigate the performance of the 15 test sections at the Florida SPS-5 project site from 1995 to 2014. The study also considers the effects of unusually high moisture on the performance of the test sections due to extreme rain events, such as hurricanes and tropical storms.

Table 1. Florida SPS-5 test section overview.

Surface Preparation	Overlay Material	Overlay Thickness	Test Section
Routine Maintenance (Control)	-	0 in	121030
Minimum	Recycled AC	2 in	120502
		5 in	120503
	Virgin AC	2 in	120505
		5 in	120504
Intensive	Recycled AC	2 in	120506
		5 in	120507
	Virgin AC	2 in	120509
		5 in	120508
Supplemental Sections	Recycled AC	3.5 in (overlay)	120561
		3.5 in (mill/inlay)	120565
		2.7 in (mill/inlay)	120564
	Virgin AC	3.5 in (overlay)	120562
		3.5 in (mill/inlay)	120566
		2.6 in (mill/inlay)	120563

SITE DESCRIPTION

The 15 LTPP SPS-5 test sections are located on US Route 1, southbound, in Martin County, Florida. US Route 1 is a rural principal arterial with two lanes in each direction of traffic. It is classified as being in a wet – no freeze climate zone with an average annual precipitation ranging between 28.9 inches (2000) and 72.7 inches (1995) during the performance period in question (1995 to 2014). The coordinates of the test l sections are provided in Table 2. Attachment A shows photographs of the test sections at Station 0+00 looking in the direction of traffic in 2014. Maps 1 and 2 show the geographical location of the test sections relative to Fort Lauderdale, Florida, and to the other test sections, respectively.

Table 2. Coordinates of test section locations.

Test Section	Latitude	Longitude
40_0502	27.03852	-80.11327
40_0503	27.03037	-80.11075
40_0504	27.01133	-80.10348
40_0505	27.00665	-80.10162
40_0506	27.01802	-80.10637
40_0507	27.0136	-80.1045
40_0508	27.02818	-80.11015
40_0509	27.02057	-80.10742
40_0561	27.0327	-80.11148
40_0562	27.00902	-80.10255
40_0563	27.00127	-80.09925
40_0564	26.999	-80.09835
40_0565	27.02292	-80.10842
40_0566	27.01592	-80.10547
40_1030	26.9949	-80.09662

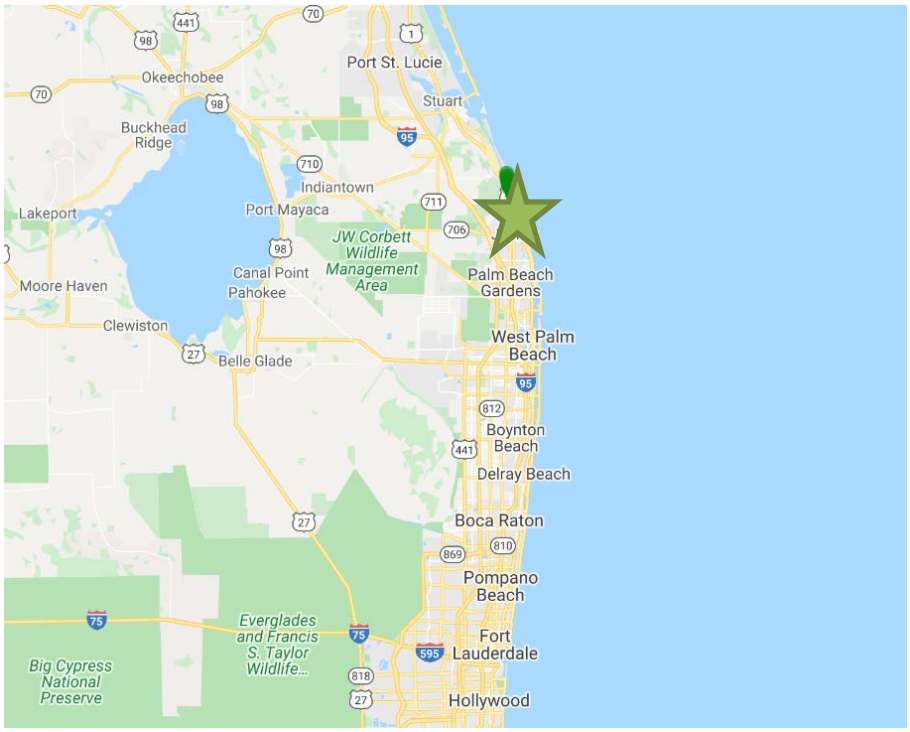

Map 1. Geographical location of test section relative to Fort Lauderdale, Florida.

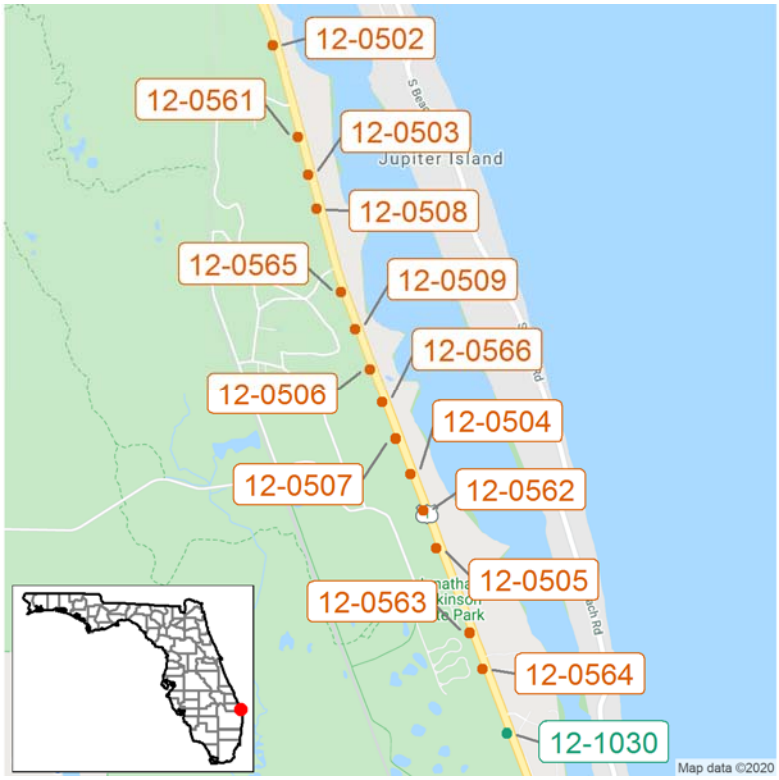

Map 2. Location of LTPP sections included in study.

PAVEMENT HISTORY

This section of the document presents historical data on the pavement structure, pavement deflection response, climate, traffic and pavement distresses.

Pavement Structure and Construction History

The original pavement structure was constructed in 1971. The pavement structure from sampling measurements performed at each test site and the control site is summarized in Table 3. The initial pavement structure consisted of a semi-infinite untreated coarse grained soil with poorly graded sand subgrade layer, an unbound granular subbase, an unbound granular base layer, a dense graded AC layer, and an open graded surface coarse layer. It is interesting to note that the unbound subbase and base layers had greater thickness uniformity across the site than the AC layers.

A second construction event took place in April 1995 (CN = 2), when the overlays on the SPS-5 test sections were placed. On this test site, the existing pavement surface was milled and overlaid with hot-mix AC of varying thickness, and the AC shoulder of the test sections was replaced. Seven test sections received overlays containing AC mixes with RAP and seven test sections had virgin AC mixes that contained no RAP. Table 4 provides a summary of the variation among the sections. The additional layers added to the pavement structure during this event are summarized in Table 5 for sections receiving RAP overlays and Table 6 for sections receiving virgin AC overlays. The final construction event (CN = 3) took place in July 2014 when the existing pavement was milled and received a 2-inch overlay of hot-mix recycled AC, moving the test sections to the GPS-6S experiment; i.e., they have been retained in the LTPP program, but do not have the SPS-5 experiment designation associated with them because of the second overlay event.

Table 3. Original pavement structure during CN=1, prior to overlay.

Layer #	Layer Type	Material Code Description	Layer Thicknesses (in.) for Test Sections 12_05**													
			01[1]	02	03	04	05	06	07	08	09	61	62	63	64	65	66
1	Subgrade (untreated)	202-Coarse-Grained Soils: Poorly Graded Sand															
2	Unbound (granular) base	308-Soil-Aggregate Mixture (Predominantly Coarse-Grained)	17.1	18.0	17.0	17.0	18.0	17.0	17.0	17.0	18.0	18.0	18.0	18.0	18.0	17.0	17.1
3	Unbound (granular) base	303-Crushed Stone	9.8[2]	8.8	10.7	10.0	8.8	10.0	9.0	10.0	8.8	8.8	8.8	8.8	8.8	10	9.8
4	Asphalt concrete layer	1-Hot Mixed, Hot Laid AC, Dense Graded	3.3[3]	3.1	2.4	2.9	2.9	3.0	2.8	2.8	3.2	2.1	2.7	3.0	3.1	3.1	2.8
5	Asphalt concrete layer	2-Hot Mixed, Hot Laid AC, Open Graded	-	0.3	1.6	0.1	0.4	1.4	0.3	0.5	0.5	0.9	0.1	0.2	0.2	0.1	0.5

[1]12_0501 is the control section; also named section 12_1030.

[2]While this layer is classified as a soil aggregate mixture, predominately coarse grained in the LTPP database; from the lab test results, it appears to be identical to material in this layer on the other test sites at this location.

[3] It appears that what is reported as an open graded surface course on the other SPS-5 test sections at this site, was combined into a single AC structural layer on the control section.

The control section is located near the test sections on the same route and has a similar pavement structure. In the initial pavement structure characterization, it appears that what is reported as an open graded surface course on the other SPS-5 test sections at this site, was combined into a single AC structural layer on this test section. Three construction events are recorded for this pavement test section over time. When it was accepted into the LTPP program in the GPS-1 experiment, the pavement layer and consisted of four layers—subgrade, subbase, base, and an asphalt concrete layer as depicted in Table 3. In 1993, the control section underwent a second construction event (CN=2) where the AC shoulder was replaced. A third construction event occurred in July 2014 when the section was milled and overlaid with hot-mix recycled asphalt.

As depicted in Tables 3 through 6, the AC overlay received by each of the test sections varied by thickness, milling depth, and material type while the material properties of the base, subbase and subgrade soil layers were similar across all test sections. It is worth noting from Table 3 that the original pavement structure had a relatively thin (3 to 4 inches) AC layer. It is also worth noting that the open graded surface course varied between 0.1 to 0.5 inches on all the test sections except the control test section. Judging by photographs of the control test section, it also had an open graded surface course, but was not noted in the original LTPP core examination that was used to determine layer thicknesses. Table 4 shows the history of the change in the pavement structure due to milling and addition of new pavement layers. Table 5 shows the layer structure of the new pavement materials applied to the test sections with RAP overlay layers. Table 6 shows the layer structure of the new pavement materials applied to the test sections with virgin AC overlay layers. Note that the thickness of the individual overlay layers were combined in the analysis presented in this memorandum.

Table 4. Change in pavement structure due to milling an addition of new pavement layers.

SHRP ID	AC Thickness before (in)	AC Mill (in)	AC Overlay (in)	AC Thickness after (in)	Number of AC Overlay Lifts	AC Type
12_0502	3.4	-1.4	2.3	4.3	3	recycled
12_0503	4.0	-1.5	5.5	8.0	3	recycled
12_0504	3.0	-0.8	5.4	7.6	3	virgin
12_0505	3.3	-1.2	2.6	4.7	3	virgin
12_0506	4.4	-2.7	3.5	5.2	3	virgin
12_0507	3.1	-2.6	7.1	7.6	3	virgin
12_0508	3.3	-2.7	7.5	8.1	3	recycled
12_0509	3.7	-3.0	4.5	5.2	3	recycled
12_0561	3.0	-0.9	4.4	6.5	3	recycled
12_0562	2.8	-0.9	4.0	5.9	3	virgin
12_0563	3.2	-2.6	2.7	3.3	3	virgin
12_0564	3.3	-2.7	2.4	3.0	3	recycled
12_0565	3.2	-2.7	6.2	6.7	4	recycled
12_0566	3.3	-3.0	5.9	6.2	4	virgin
12_1030	3.3	0.0	0.0	3.3	0	control

Table 5. New layers added during CN=2 for sections that received RAP overlay.

Layer #	Layer Type	Material Code Description	Thickness (in.) for Test Sections 12_05**						
			02	03	08	09	61	64	65
6	Asphalt concrete layer	Recycled AC, Hot Laid, Central Plant Mix	1.3	2.7	2.6	3.1	2.9	1.4	2.6
7	Asphalt concrete layer	Recycled AC, Hot Laid, Central Plant Mix	0.7	2.4	4.4	1	1	0.6	2.1
8	Asphalt concrete layer	Hot Mixed, Hot Laid AC, Open Graded	0.3	0.4	0.5	0.4	0.5	0.4	1.1[1]
9	Asphalt concrete layer	Hot Mixed, Hot Laid AC, Open Graded	NA	NA	NA	NA	NA	NA	0.4

[1]Used -Recycled AC, Hot Laid, Central Plant Mix instead of Hot Mixed, Hot Laid AC, Open Graded.

Table 6. New layers added during CN=2 for sections received virgin AC.

Layer #	Layer Type	Material Code Description	Thickness (in.) for Test Sections 12_05**						
			04	05	06	07	62	63	66
6	Asphalt concrete layer	1-Hot Mixed, Hot Laid AC, Dense Graded	3.5	1.3	1.9	2.1	2.6	1.3	2.3
7	Asphalt concrete layer	1-Hot Mixed, Hot Laid AC, Dense Graded	1.5	0.8	1.1	4.5	0.9	0.9	2.2
8	Asphalt concrete layer	2-Hot Mixed, Hot Laid AC, Open Graded	0.4	0.5	0.5	0.5	0.5	0.5	1.0
9	Asphalt concrete layer	2-Hot Mixed, Hot Laid AC, Open Graded	NA	NA	NA	NA	NA	NA	0.4

Pavement Structural Properties

Figure 1 shows the average Falling Weight Deflectometer (FWD) deflection under the nominal 9,000-pound load plate over time for each test section; Figure 1.a shows the deflections for the six core test sections and control section, while Figure 1.b shows the deflections for the supplemental test sections and control test section. The deflection of the sensor located in the center of the load plate is a general indication of the total "strength" or response of all layers in the pavement structure to a vertically applied load. This deflection can be influenced by pavement temperature at the time of testing, precipitation, and changes in pavement structure.

As shown in Figure 1, the measured deflections ranged between 6.8 mils (section 12_0565) and 9.9 mils (section 12_0564) in 1994 prior to the application of the overlays. After the application of the first AC overlay in 1995, the deflections for all sections appear to have decreased, including the control test section, which did not receive an overlay. Between 1995 and 2004, the deflections observed on all sections remains relatively consistent, with slight variations in the deflections reported. The variations are consistent with the variability of temperatures during testing dates. By 2009, the deflections observed on most sections increased with values ranging from 4.6 mils to 10 mils in 2009. The deflections observed on the test sections in October 2013, prior to the second overlay ranged between 5.0 mils (section 12_0507) and 9.0 mils (section 12_0563). The control section 12_1030, which did not receive an overlay, appears to have higher deflections than the other site test sections, with an average deflection of 10 mils in 2009.

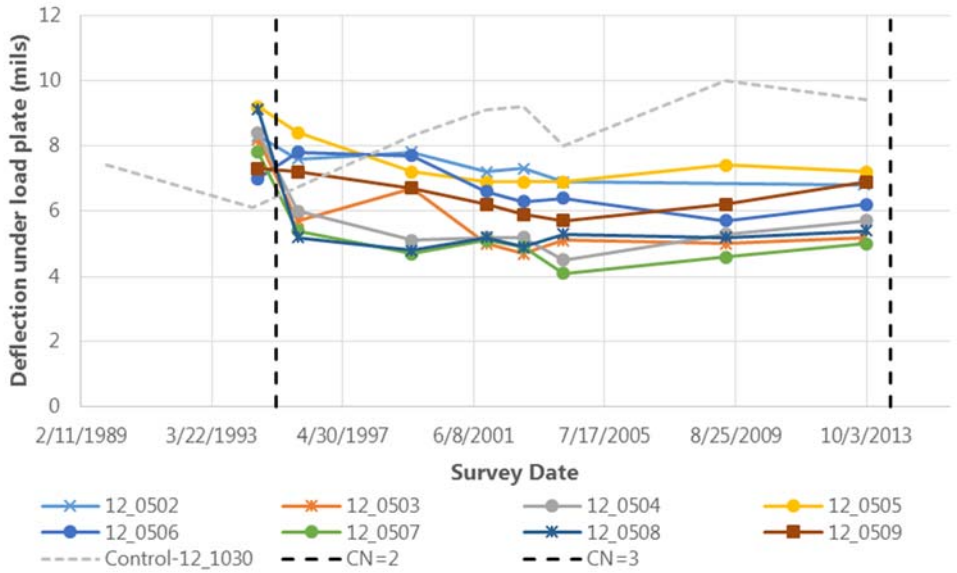

a. Core Test Sections

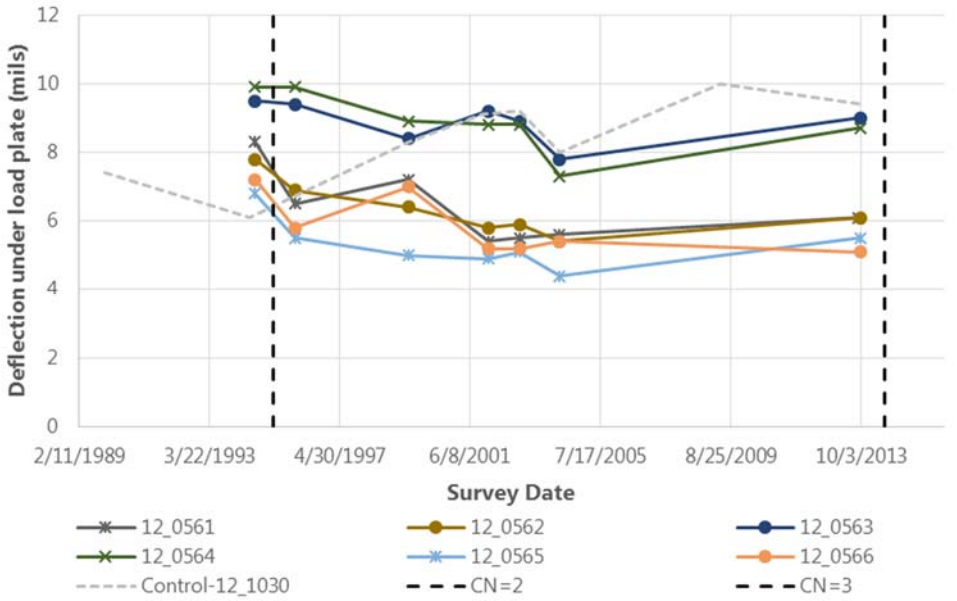

b. Supplemental Test Section

Figure 1. Average deflection for the sensor located in the load plate normalized to 9,000 lb. drop load over time.

In reviewing Figure 1, the following additional observations can be made:

- The range in deflection over time is relatively small. Differences of this magnitude could easily be due to changes in the temperature of the AC layer at the time of testing.
- In general, the thicker the AC layer following overlay placement, the lower the measured deflection response.
- The type of AC overlay mix (virgin versus RAP) a section received did not seem to play a role in measured deflection response.

Climate History

The monthly and annual average precipitation for the test sections between 1994 and 2014 are shown in Figure 2. The period of interest for this study is between 1995 and 2014. The average annual amount of precipitation reported at the sections had a large spread; the reported annual precipitation ranged from 28.9 in. in 2000 to 72.7 in. in 1995. The variability in annual average precipitation reported each year is largely related to the extreme weather events, such as hurricanes and tropical storms. Over the life of the Florida SPS-5, the test sections were subjected to the several of these major rain events including named hurricanes and tropical storms. For example, the hurricanes included Keith and Chris in 1988, Ana in 1991, Gordon in 1994, Jerry and Erin in 1995, Mitch in 1998, Harvey and Irene in 1999, Ivan, Frances and Jeanne in 2004, Ophelia, Wilma, Katrina and Tammy in 2005, Ernesto in 2006, Andrea in 2007, Fay in 2008, Nicole and Bonnie in 2010, Dorian in 2013 and Arthur in 2014.

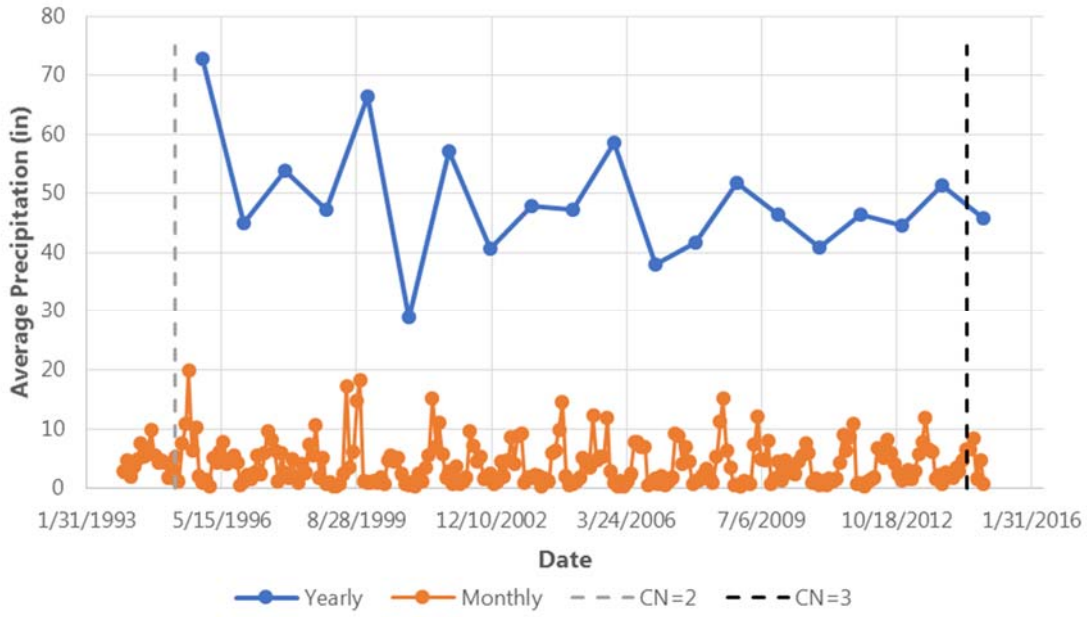

Figure 2. Average monthly and annual precipitation over time.

In terms of precipitation observed following the application of the AC overlays in 1995, a spike in the average annual precipitation was observed in 1995 and 1999 where 72.7 in. and 66.4 in. of precipitation were reported, respectively. The spikes may be related to the weather events that occurred during these years: Hurricane Erin and Tropical Storm Jerry in 1995 and Hurricane Irene and Tropical Storm Harvey in 1999. For example, the average monthly precipitation in August 1995 was 19.9 inches and in October 1999 it was 18.2 inches. The increase in precipitation observed on these sites likely had an impact on the performance of the test sections and will be explored further in subsequent sections. It should be noted that the unbound pavement layers at this site are largely coarse grained which are typically associated good drainage

While the average precipitation reported at the sections likely plays a role in the sections' performance, the freezing index does not, as would be expected for Florida. The sections in this project are in a no freeze climate and the reported freezing index for the site is zero.

Truck Volume History

Figure 3 shows the computed or estimated annual average daily truck traffic (AADTT) in the LTPP test lane for all sections by year (derived from the TRF_TREND table). The counts reported were a combination of

counts calculated using a compound growth function (1971-1988 and 2009-2017), historical AADTT (1989), state provided AADTT (1990, 1996, and 2001), monitored AADTT (1991, 1992, and 1997), and calculated from monitored Class data (1993-1995, 1998-2000, and, 2002-2009). The AADTT was reported for the test sections between 1971 and 2017 and shows an overall decrease in truck traffic over time. Initially, 431 trucks/day were observed on the site locations in 1971. By 2017, the number of trucks observed had decreased to 149/day, nearly a 65% decrease in truck traffic since 1971. While there is an overall decrease in trucks, there is variability in the truck traffic reported, as can be observed by the 1989 and 1990 count spikes. These spikes may be attributed to the source of the estimated AADTT data as 1989 represents a historical AADTT value and 1990 was a state provided value.

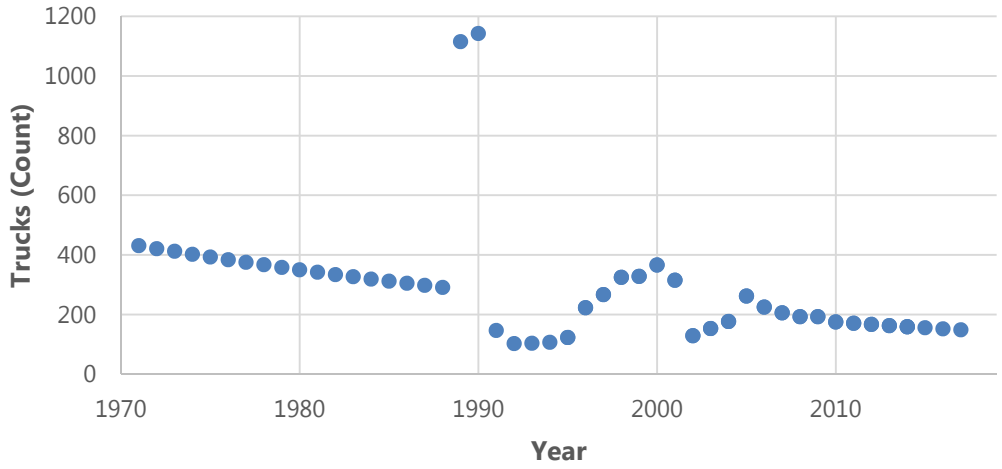

Figure 3. Average annual daily truck traffic (AADTT) history.

Pavement Distress History

The following sections summarize the distresses observed on the 15 SPS-5 project test sections between 1993, which is the last survey prior to the test section becoming part of the SPS-5 project, and 2013, which is when the last manual distress survey was performed as part of the SPS-5 project performance period. The specific distresses assessed were fatigue cracking, longitudinal cracking, transverse cracking, IRI, and rutting. No block cracking or patching was observed.

Fatigue Cracking

Fatigue cracking performance was evaluated as the progression of alligator cracking (FCRK) over time. The FCRK measurements used in the analysis consisted of the total area of alligator cracking measured for the section, computed as the sum of alligator cracking areas for low, medium and high severity levels. Note that in the LTPP database, fatigue cracking is not defined to occur in the wheel paths thus there is some question if it represents the traditional bottom-up or top down fatigue cracks used in mechanistic based AC pavement distress models. Figure 4 shows the FCRK values over time before and after the application of the AC overlay in 1995, while Figure 5 shows the FCRK values over time for only the analysis period of interest – 1995-2014.

Figure 4 shows that nine of the test sections had fatigue cracking before application of the 1995 AC overlay, with some test sections reporting values greater than 2,000 ft^2. This was considered relevant to the study and therefore this factor was taken into consideration as those test sections with higher amounts of alligator-fatigue cracking prior to the overlay were considered more prone to the earlier appearance of cracks on the surface after application of the overlay. It is interesting that the control test section, unlike the other test sections at the site, did not exhibit any fatigue-alligator cracking until 2009. It did however

experience significant block cracking, which can be a mixture of different types of cracks and confound distress analysis based on separate distress data.

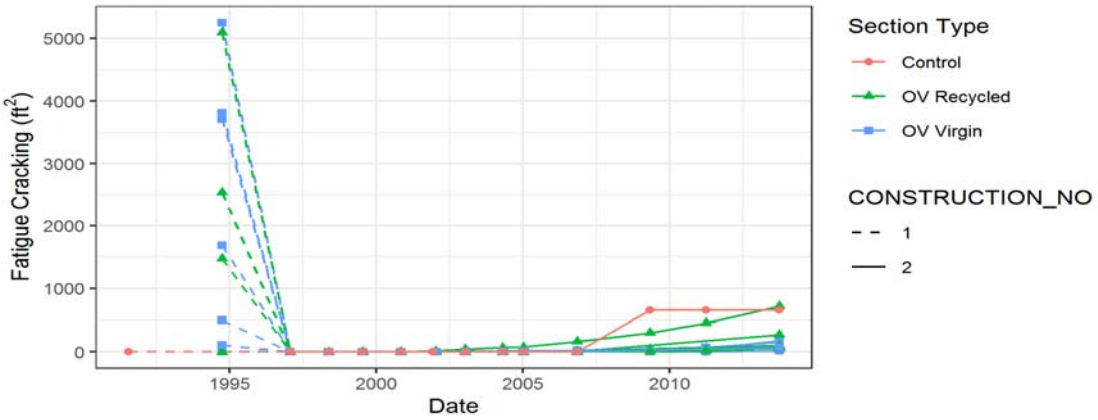

Figure 4. Fatigue cracking measurements before and during SPS-5 experiment.

Figure 5 shows that the test sections after placement of the 1995 AC overlay vary in terms of the number of years for FCRK initiation. Two sections (SHRPs 0502 and 0561) appear to deteriorate at a faster rate, while the performance curve for the control section shows a sudden increase in FCRK after 2007 while all other test sections show a smooth progression of FCRK over time. This cracking increase on the control test section might have been the progression of block cracking to smaller alligators cracks. It is also worth noting that except for the three referenced test sections, the FCRK values are relatively low for the remaining test sections.

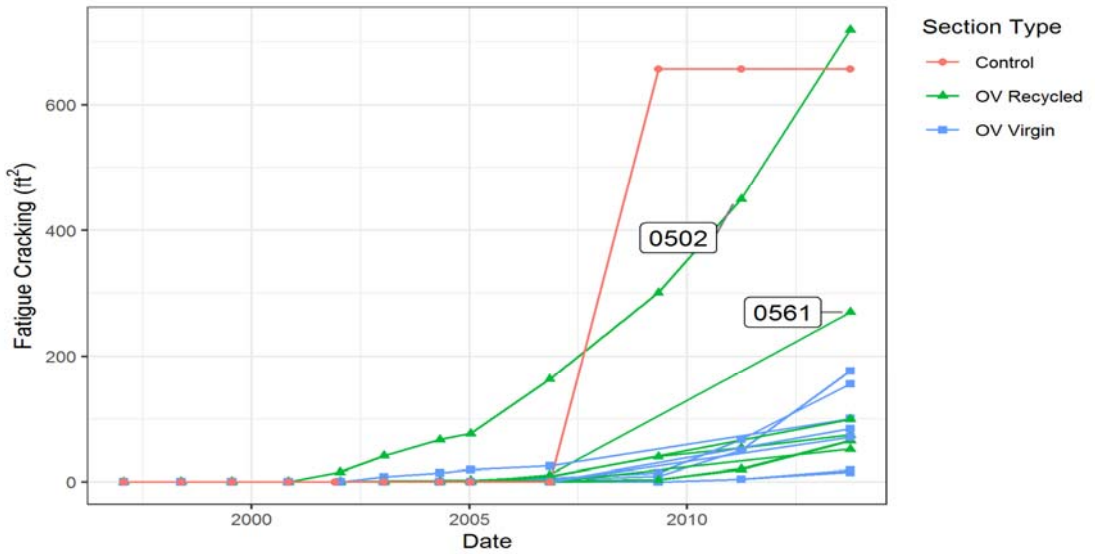

Figure 5. Fatigue cracking measurements during SPS-5 experiment.

Fatigue Cracking Initiation Model

A fatigue/alligator cracking initiation model was used to assess the effect of the overlay treatment factors on the time it took for fatigue cracking to develop on the pavement surface. The model was estimated using quantile linear regression to reduce the impact of outliers given the small sample size (14 treated sections) – control section was excluded from the overlay analysis because it did not receive an overlay,

which could bias the resulting model). The estimated model coefficients are presented in Table 7, where OV_{tot} is the total AC overlay thickness (in inches), $FCRK_{pre}$ is the FCRK area (in ft^2) before applying the overlay, AC_{rem} is the total thickness (in inches) of pre-existing AC layers after milling, and $Virgin$ is an indicator equal to 1 when overlay used virgin aggregates and 0 when overlay used recycled aggregates.

Table 7. Estimated coefficients of fatigue cracking initiation model.

Variable	Estimate	Std. Error	p-value
Intercept*	2.570e+00	1.417e+00	0.103
OV_tot	1.115e+00	1.886e-01	0.000
Virgin	2.069e+00	6.170e-01	0.008
AC_rem	1.051e+00	6.969e-01	0.166
FCRKpre	2.781e-04	1.597e-04	0.116

* Intercept represents the predicted median number of years until fatigue cracking initiation for the case of OV total thickness tended to zero, when the OV used recycled aggregates, complete removal of pre-existing AC layers after milling, and zero measured FCRK area before applying the OV. Given that the case for which all variables in the model are equal to zero does not have any practical value (and it is outside of the range of the values the model should be used for), the isolated intercept value does not provide any meaningful interpretation.

The p-values reported in Table 7 indicate that OV_{tot} and $Virgin$ were statistically significant. Each additional inch of overlay delayed the initiation of FCRK by, in average, 1.1 years, while using virgin aggregates in the overlay delayed the initiation of FCRK by, in average, 2.1 years. AC_{rem} and $FCRK_{pre}$ were not statistically significant. Therefore, the number of years since overlay application until fatigue cracking is observed on the surface was related to the thickness and materials used in the overlay, but not the pre-existing FCRK or the milling depth.

Fatigue Cracking Propagation Model

Figure 6 shows the fatigue/alligator cracking performance curves after cracking initiation. A propagation model was estimated to assess the effect of the different overlay treatment factors on the deterioration rate after crack initiation. This model was specified as an exponential model and included only overlaid test section data (i.e., no control test section data – Figure 6 shows actual measurements for this section).

The model was estimated as a mixed linear model with random effect for the intercept and the age variable. The estimated model coefficients are presented in Table 8, where AGE_{prop} is the number of years since crack initiation, $Mill_tot$ is the total milling depth (in inches), AC_rem is the total thickness (in inches) of pre-existing AC layers after milling, $and\ CRKini$ is the number of years since overlay application until fatigue cracking shows in the surface. The explanatory variables in the final model were selected through the stepwise regression iterative method, which leads to the best performing model with the available variables.

The p-values reported in Table 8 indicate that $Mill_{tot}$, AC_{rem}, and $CRKini$ were the variables with a statistically significant effect on the deterioration rate. The effects of AC_{rem}, and $CRKini$ were positive; the higher the total thickness of pre-existing AC layers after milling and the greater the number of years until

fatigue cracking shows, the faster the fatigue growth rate. On the other hand, the greater the milling depth ($Mill_{tot}$), the slower the fatigue cracking growth rate.

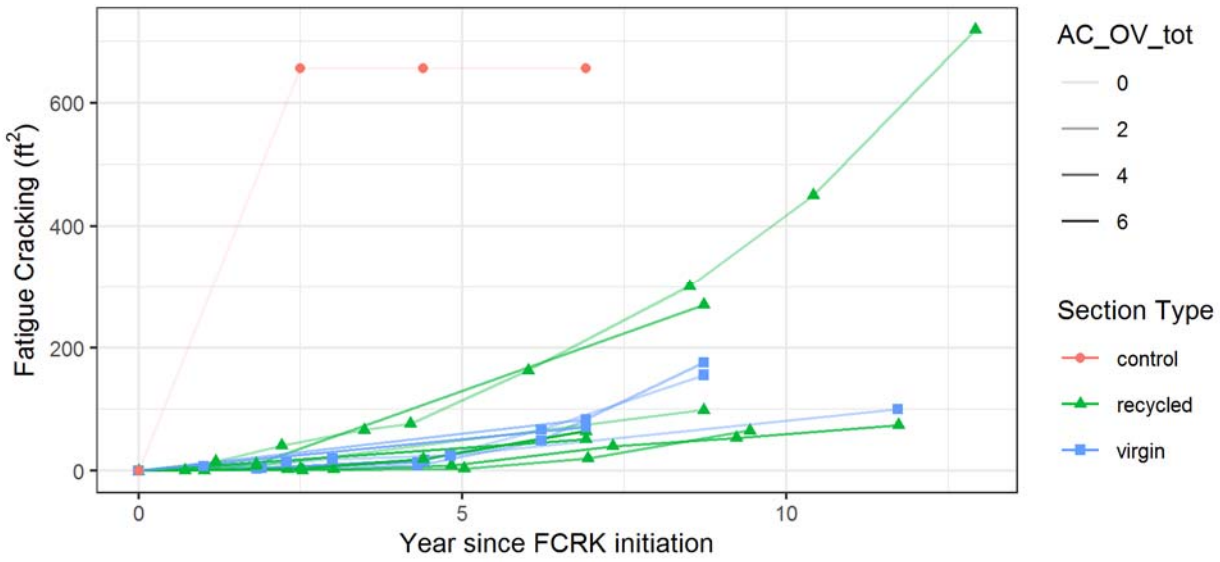

Figure 6. Fatigue/alligator cracking measurements in analysis dataset after crack initiation.

Table 8. Estimated coefficients of fatigue cracking propagation model.

Variable	Estimate	Std. Error	p-value
Intercept*	9.714e+00	2.026e+00	0.000
AC_rem	-1.756e+00	5.053e-01	0.002
CRKini	-3.124e-01	7.785e-02	0.001
Mill_tot	1.738e+00	4.842e-01	0.001
AGE_prop	-5.490e-01	1.704e-01	0.003
AGE_prop * Mill_tot	-1.368e-01	4.748e-02	0.007
AGE_prop * AC_rem	1.774e-01	4.383e-02	0.000
AGE_prop * CRKini	5.191e-02	8.894e-03	0.000

* Intercept represents the predicted value for age after initiation equal to zero in the log scale when all other variables in the model are equal to zero. Given that the case for which all variables in the model are equal to zero does not have any practical value (and it is outside of the range of the values the model should be used for), the isolated intercept value does not provide any meaningful interpretation.

Longitudinal Cracking

With the exception of test sections 12_0507 and 12_0561, wheel path (WP) longitudinal cracking was not observed during the performance period in question. Moreover, very small amounts (less than 10 feet) of WP longitudinal cracking was observed at the two referenced test sections on a single year, and for the

remainder of the years no WP longitudinal cracking was observed. Consequently, this section deals solely with non-wheel path (NWP) longitudinal cracking, hereafter just referred to as longitudinal cracking.[3]

Longitudinal cracking performance was evaluated as the progression of the longitudinal cracking (LCRK) over time. The LCRK measurements used in the analysis consisted of the total length of non-sealed longitudinal cracking measured for the section, computed as the sum of longitudinal cracking length for low, medium and high severity levels on both the inside and outside the wheel-path. The amount of sealed cracking in the analysis data set was not significant (and hence does not affect analysis), plus the performance of sealed cracks is expected to be different than non-sealed cracks. Figure 7 shows the LCRK values over time for the test sections analyzed before and after application of the 1995 AC overlay, while Figure 8 shows the LCRK values over time for only the 1995 to 2014 SPS-5 monitoring period.

Figure 7 shows that five of the test sections presented longitudinal cracking before they were overlaid, while Figure 8 shows that there was no longitudinal cracking for at least six years (1995 to 2001) following the application of the AC overlay. Moreover, the test sections vary regarding the deterioration rate and the number of years until LCRK initiation.

Longitudinal Cracking Initiation Model

A longitudinal cracking initiation model was developed to assess the effect of the AC overlay treatment factors on the number of years until longitudinal cracking appears on the pavement surface following the overlay. Several candidate models were estimated using quantile linear regression to reduce the impact of outliers given the small sample size (14 test sections). After trying different model specifications, it was found that none of the available variables had a statistically significant effect on the time until longitudinal cracking initiation.

However, while none of the treatment factors played a significant role in the initiation of longitudinal cracking, the increase in precipitation that occurred in 1999, may have played a role. Additional analysis of the effect average annual precipitation had on the initiation and propagation of cracking is recommended.

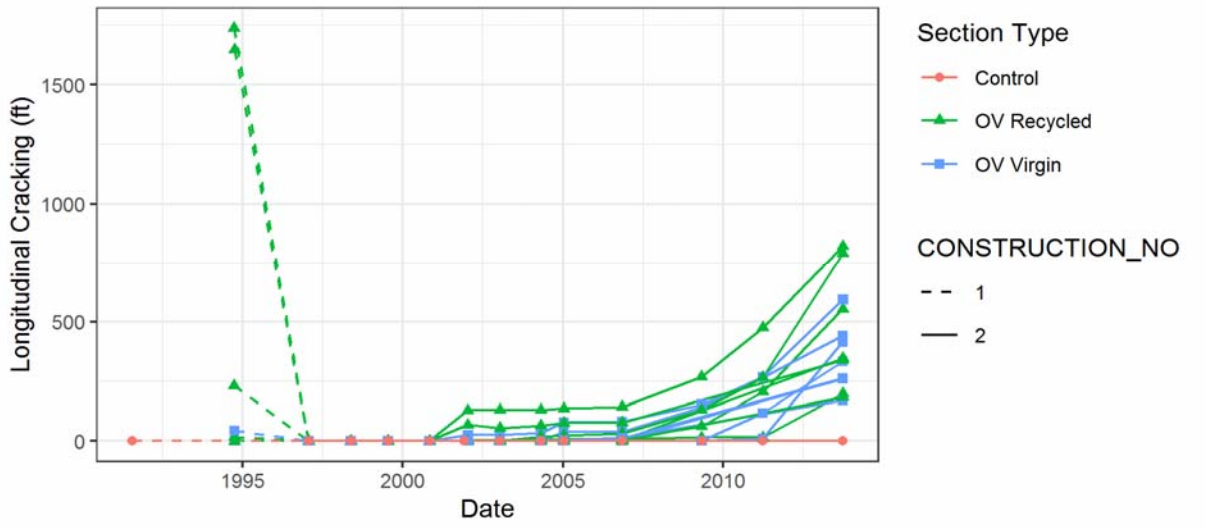

Figure 7. Longitudinal cracking measurements before and during SPS-5 experiment.

[3] NWP longitudinal cracking could have something to do with NWP alligator cracking at the test sections; longitudinal joints and precipitation (and hence possible striping of the asphalt) are potential issues. NWP alligator cracking can also be a materials issue related to bad compaction at the edges of the pavement, bad sealing of the longitudinal joints, mix segregation, or a combination of these factors.

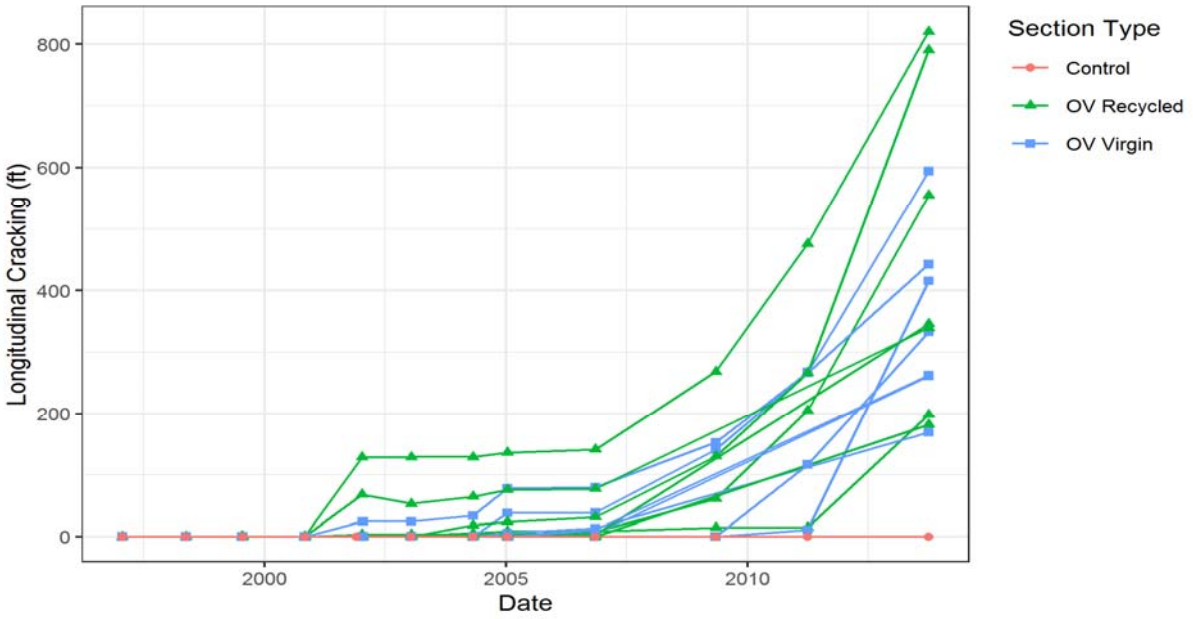

Figure 8. Longitudinal cracking measurements during SPS-5 experiment.

Longitudinal Cracking Propagation Model

Figure 9 shows the longitudinal cracking performance curves after cracking initiation. Different candidate propagation models were estimated to assess the effect of the different overlay treatment factors on the deterioration rate after crack initiation. These models were specified as exponential and included only overlaid test section data (i.e., no control test section data). After trying the different models, it was found that none of the available variables had a statistically significant effect on the deterioration rate over time of longitudinal cracking, which is likely due to the high variability in the results versus the primary experimental factors. In other words, there were no clear trends, statically or otherwise.

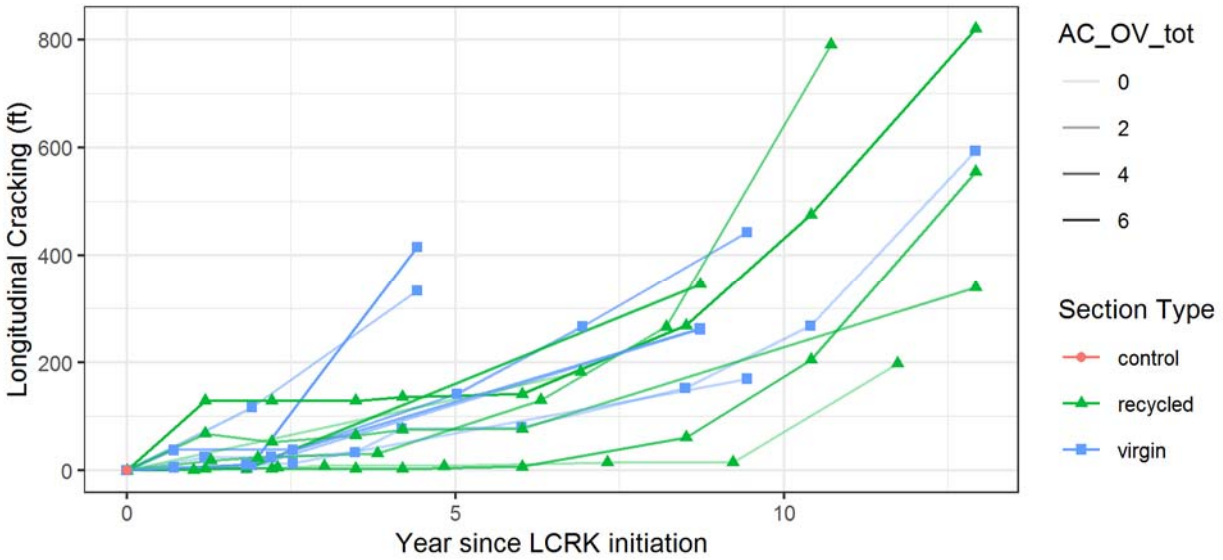

Figure 9. Longitudinal cracking measurements in analysis dataset after crack initiation.

Transverse Cracking

Figure 10 summarizes the number of transverse cracks that were observed prior to and after the application of the 1995 AC overlay. Immediately following the application of the AC overlay in 1995, no significant amount of transverse cracking was observed on the test sections. As shown in the figure, transverse cracking was relatively stable between 1995 until 2005. By 2005 or 10 years after the application of the AC overlay, the amount of transverse cracking observed slowly increased for most of the test sections. By 2013, the amount of transverse cracking observed on the test sections varied from 0 (section 12_1030) to 70 (section 12_0502).

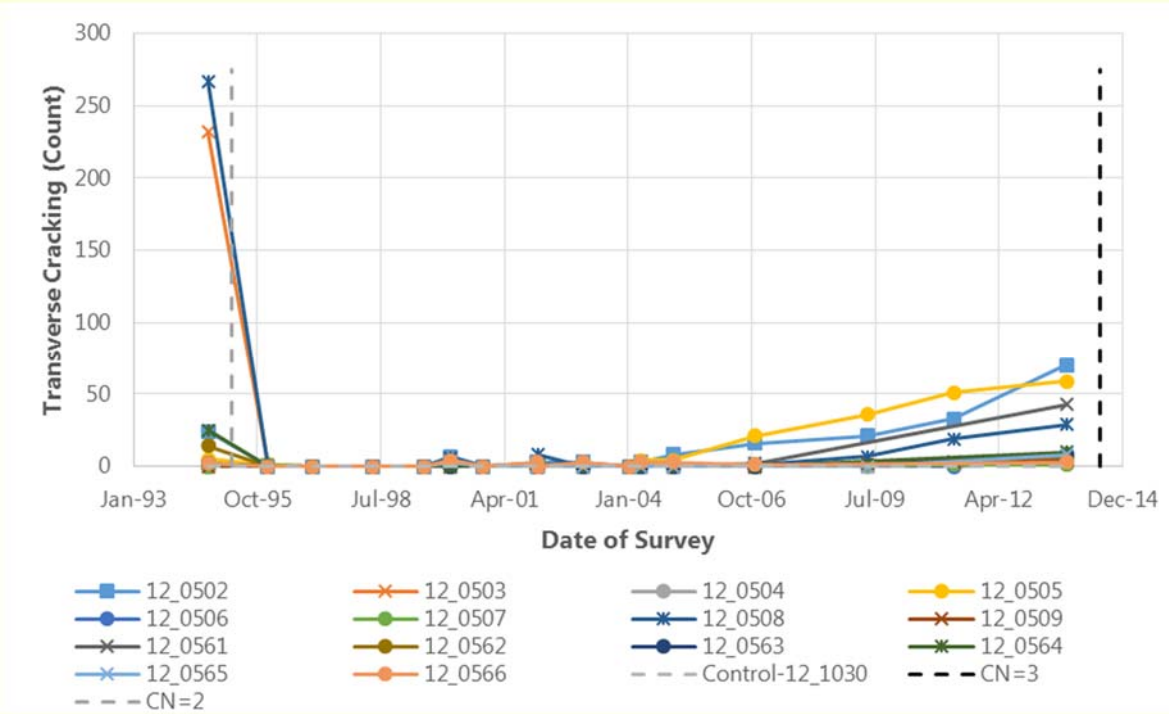

Figure 10. Time history of the number of transverse cracks.

The cause of the transverse cracking initiation and propagation remains unclear. The type and thickness of the asphalt overlay selected did not seem to play a clear role. Because transverse cracking is typically a result of environmental factors, further assessment of the climatic factors at the sites need to be investigated.

IRI

Ride performance was evaluated as the progression of IRI over time. The IRI measurements used in the analysis consisted of the mean IRI value from both wheel-paths. Figure 11 shows the IRI values over time data for the test sections in question. The solid lines connect the IRI data points collected during the 1995 to 2014 SPS-5 performance period, while the dashed lines connect the IRI data points prior to application of the AC overlay in 1995. The IRI statistical analysis was limited to those data collected during the 1995 to 2014 time period; however, data collected prior to that period provides information about the pre-existing condition of the pavement. The pink curve with round markers corresponds to the control test section, the green curve with triangular markers corresponds to test sections overlaid using RAP, and the blue curve with square markers corresponds to test sections overlaid using a virgin AC mix.

The IRI values before treatment ranged between 61.5 and 91.6 inches/mile. Figure 12 shows the distribution of the change in IRI after application of the 1995 AC overlay, grouped by the type of mix used.

The figure suggests that the test sections that the virgin AC mixtures resulted in higher reductions in IRI. Based on the p-value from a t-test between these two groups, the difference in the mean change in IRI values was statistically significant (with a 10% confidence level).

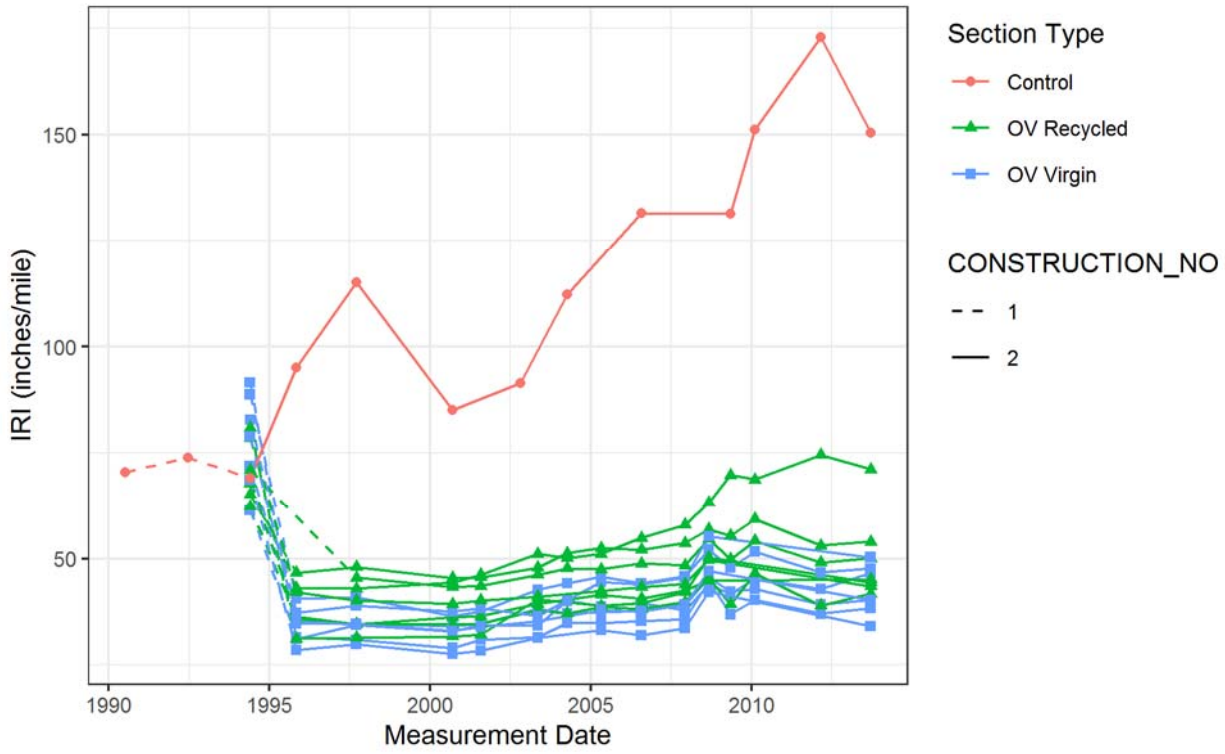

Note: the first IRI measurement for section 12-0508 (CN#2) was on September 14, 1997, whereas the first IRI measurements for all other treated sections (CN#2) was on November 2, 21995.

Figure 11. IRI measurements in analysis dataset.

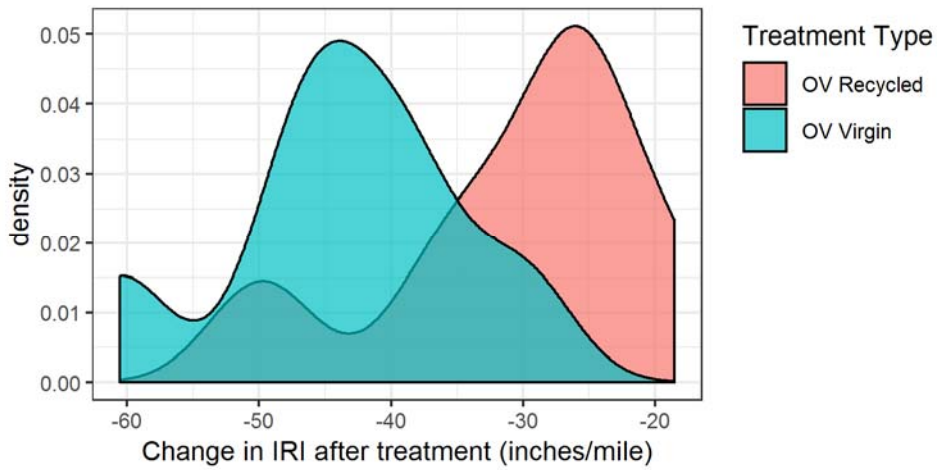

Figure 12. Distribution of drop in IRI before and after 1995 AC overlay.

Going back to Figure 11, this figure also suggests that the control test section deteriorated faster than the overlaid test sections, and that there is also a slight difference in deterioration rate between overlays using

virgin AC versus RAP mixtures. These variations in the deterioration rate may be a consequence of applying the overlays, having higher initial IRI, higher total AC thickness, or a combination of these and other factors. The analysis in the next section aims to address the effect of these factors.

IRI Model

An IRI performance model was developed using the different SPS-5 experimental factors as explanatory variables to assess their effect on the IRI deterioration rate. The final performance model was selected based on a comparison of the accuracy and complexity among different feasible model specifications. The explanatory variables in the final model were selected through the iterative stepwise regression method, which leads to the best performing model with the available variables.

The equation of the final IRI performance model is presented below, where AGE is the number of years since last surface application, $Recycled$ is an indicator variable equal to 1 when the overlay used RAP and as 0 when the overlay used virgin AC mixes, $Treated$, is an indicator variable equal to 1 when the section was treated with an AC overlay and 0 when it did not, OV_{tot} is the total AC overlay thickness (in inches), and IRI_{ini} is the IRI value at the beginning of the service life.

$$log(IRI) = \beta_o + \beta_{Treated} * Treated + \beta_{Recycled} * Recycled + \beta_{Treated\_OV_{tot}} * Treated * OV_{tot} + \beta_{AGE} * AGE + \beta_{AGE\_IRI_{ini}} * AGE * IRI_{ini} + \beta_{AGE\_Treated} * AGE * Treated + \beta_{AGE\_Treated\_OV_{tot}} * AGE * Treated * OV_{tot}$$

The model was estimated as a mixed model with random effect for the intercept and the age variable. The estimated model coefficients are presented in Table 9. The interactions between the variable AGE and the variables $Treated$, IRI_{ini}, and OV_{tot} were found to have a statistically significant effect on the deterioration rate. Higher initial IRI values or lower total overlay thickness values resulted in a higher deterioration rate, as expected. Since sections treated with AC overlays using virgin AC mix had lower initial IRI values, their resulting deterioration rates were lower. Although these effects were statistically significant, their magnitude were found to be moderate.

Table 9. Estimated coefficients of IRI performance model.

Variable	Estimate	Std. Error	p-value
Intercept	4.339e+00	1.076e-01	0.000
Recycled	1.304e-01	5.407e-02	0.029
Treated	-1.045e+00	1.379e-01	0.000
Treated * OV_tot	3.920e-02	1.653e-02	0.030
AGE	8.376e-03	1.195e-02	0.484
AGE * IRI_ini	4.140e-04	1.648e-04	0.013
AGE * Treated	1.320e-02	7.210e-03	0.069
AGE * Treated * OV_tot	-4.040e-03	4.870e-04	0.000

Rutting

Rutting performance was evaluated as the progression of the section rut depth (RUT) over time. The RUT measurements used in the analysis were the maximum of the two wheel-path RUT mean values. More specifically, the rut statistic used was MAX_MEAN_DEPTH_1_8, which represents the maximum value of the

left or right lane half 6-foot straight edge depth mean. Figure 13 shows the RUT values over time data for all analyzed sections. Note that in the LTPP database, rut depths are reported in increments of 1 mm.

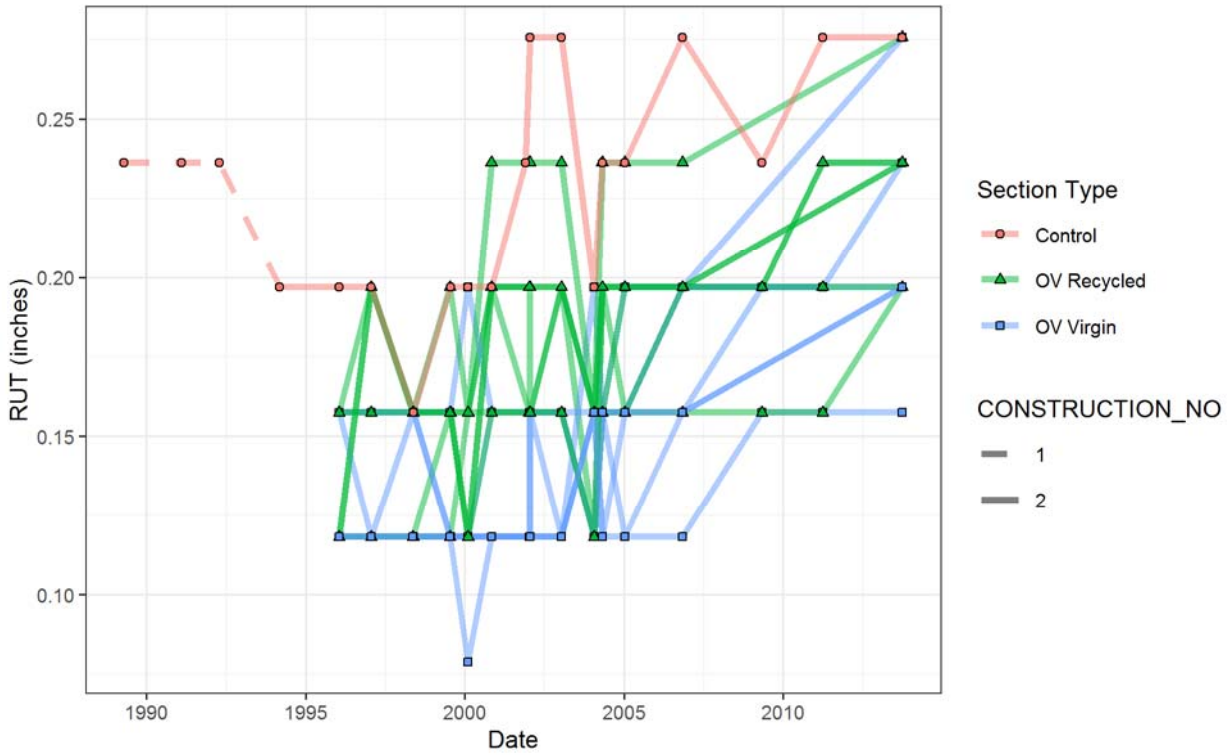

Figure 13. Rutting measurements in analysis dataset.

The solid lines connect the RUT data points collected during the 1995 to 2015 SPS-5 performance period, while the dashed line connects the RUT data points collected prior to the 1995 AC overlay on the control section. As shown in this figure, only the control section had rutting measurements available before the 1995 AC overlay. The dotted (pink) curve corresponds to the control test section, the triangular (green) curve corresponds to the SPS-5 test sections with AC overlay that used recycled aggregates, and the square (blue) curve corresponds to the SPS-5 test section with AC overlay using virgin aggregates.

Figure 13 shows that none of the test sections reported significant rutting. Both the rutting values and the increase in rutting over the analysis period were not high. The performance curves in the figure show a drop in RUT value after application of the AC overlay; however, this drop does not appear to vary significantly. Both groups of test sections (virgin and recycled mixes) had an initial RUT value lower than the one for the control test section by 0.06 inches on average. Given the observed low magnitude and variability of rutting, no further analysis was performed on this condition metric.

SUMMARY OF FINDINGS

In this memorandum, information concerning the performance history of fourteen test sections and one control test section that make up the SPS-5 project in Martin County, Florida was explored. The LTPP SPS-5 experiment is a study of asphalt concrete (AC) overlay on AC pavements. The test sections at the Florida SPS-5 project were subject to similar climatic, subgrade, and traffic conditions and they had similar pavement structures. The experimental factors that were the focus of this desktop study were mix type (virgin AC versus RAP mixes), surface conditions prior to overlay, surface preparation and overlay thickness.

Through this technical memorandum, the following information about the performance of the sections was presented:

- ***Deflections***: After the application of the first AC overlay in 1995, the deflections for all sections decreased. There was a modest decrease in deflections on the control section that is indicative of the temporal changes in the pavement structure caused by temperature or moisture affects. By 2009, the deflections observed on most sections increased with values ranging from 4.6 mils to 10 mils in 2009. Overall, the deflections observed are small for an AC pavement structure, which is appears to be related to the foundation structure of the base and subbase layers. In general, the thicker the AC layer following overlay placement, the lower the measured deflections the test sections. Additionally, the type of mix used in the AC overlay did not appear to play a role in the deflection response measurements.
- ***Fatigue/Alligator Cracking*:** Fatigue/alligator cracking was observed before each test section was overlaid, some sections reporting cracking values greater than 2,000 ft^2. Following application of the overlay, fatigue/alligator cracking initiation varied with two sections showing a sudden increase after 2007, while the remaining test sections showed a smooth progression. The thickness and materials used in the overlay played a significant role in the initiation of fatigue/alligator cracking, while the pre-existing cracking and the milling depth did not. The total thickness and number of years since the overlay was applied until fatigue/alligator cracking developed had a positive relationship with the propagation of f cracking. In other words, the higher the AC thickness after milling (but prior to overlay) or the greater the number of years to fatigue/alligator cracking initiation, the faster the fatigue/alligator cracking growth rate. On the other hand, the deeper the milling depth, resulted in a slower fatigue/alligator cracking growth rate.
- ***Longitudinal Cracking*:** After the test sections were overlaid, WP longitudinal cracking was only observed on two test sections, but very small amounts (less than 10 feet) and in just one year. Consequently, the study focused solely on NWP longitudinal cracking. No NWP longitudinal cracking was observed for at least six years. The overlaid test sections vary regarding the deterioration rate and the number of years before crack initiation. While none of the treatment factors played a significant role in the initiation or propagation of NWP longitudinal cracking, the substantial precipitation that occurred in 1999 may have played a role in the amount of NWP longitudinal cracking.
- ***Transverse Cracking*:** Transverse cracking was relatively stable between the application of the AC overlay in 1995 until 2005. By 2005, the amount of transverse cracking observed slowly increased for most of the test sections. While the cause of the transverse cracking initiation and propagation remains unclear since this site is located in a no-freeze zone, some LTPP studies have indicated that repeated truck wheel loading associated with fatigue type cracking mechanism appears to influence the increase in transverse cracking[4]. The type and thickness of the asphalt overlay selected did not seem to play a clear role in this distress mechanism.
- ***IRI:*** IRI values before treatment ranged between 61.5 and 91.6 inches/mile. Following the overlay, higher initial IRI values and lower total AC overlay thickness values resulted in higher deterioration rates in IRI, as expected. Since test sections with AC overlays using virgin mixes had lower initial IRI values, their deterioration rates were lower. Although these effects were statistically significant, their magnitudes were found to be moderate.

[4] Leslie Titus-Glover, M. Darter, Harold Von Quintus (2019). *Impact of Environmental Factors on Pavement Performance in the Absence of Heavy Loads*, McLean, VA, Federal Highway Administration.

- ***Rutting*:** None of the analysis test sections reported significant rutting. Both the rutting values and the increase in rutting over time were not high. The performance curves showed a drop in rut depth values after applying the 1995 AC overlay; however, this drop in the deterioration rate did not appear to vary significantly.

The results of this study were also compared two national studies on the topic: FHWA-HRT-10-066 *Statistical Analysis of Performance of Recycled Hot Mix Asphalt Overlays in Flexible Pavement Rehabilitation* and FHWA-RD-01-168 *Rehabilitation of Asphalt Concrete Pavements: Initial Evaluation of the SPS-5 Experiment—Final Report*. The comparison findings are summarized below:

- ***Deflections*:** In a consolidated analysis (using a Friedman test for all SPS-5 test site data) of the effect of rehabilitation strategies on the structural response of a pavement, Report FHWA-HRT-10-066 found that thicker overlays provided lower maximum deflections when compared to thin overlays. The study also summarized the effect climate, traffic, and surface condition has on the deflections reported. For wet, no-freeze sites with low traffic and poor pavement conditions, such as Florida sites, the Friedman test ranked milled pavement with a thick virgin overlay as the best treatment strategy for low deflections. These findings are partially aligned with the findings of this desktop study where thicker overlays resulted in lower deflections. However, this desktop study did not find the type of AC overlay to play a significant role in the deflections reported.
- ***Fatigue Cracking***: In the FHWA-HRT-10-066 Report, a Friedman test was used to rank rehabilitation strategies in terms of fatigue cracking performance. The study found that milling with thick virgin overlays yielded the best fatigue cracking performance (in terms of weighted distress or unit area under the distress performance curve) in the long-term, especially when considering the traffic and climate conditions for the Florida sites. In the FHWA-RD-01-168 Report, it was noted that in the short term, based on an analysis of variance (ANOVA), fatigue cracking was most affected by age, temperature, and moisture of the test sites. Through the desktop study, the thickness and type of overlay used were found to most affect the crack initiation rate, while the thickness and age when fatigue cracking first appeared, and milling depth affected growth rate.
- ***Longitudinal Cracking***: In the FHWA-HRT-10-066 Report, a Friedman test was used to rank rehabilitation strategies in terms of longitudinal cracking performance. The study found that milling with thick virgin overlays yielded the best longitudinal cracking performance (in terms of weighted distress or unit area under the distress performance curve) in the long-term, especially when considering the traffic and climate conditions for the Florida sites. In the desktop study, the overlaid test sections varied in terms of the deterioration rate and the number of years before crack initiation of longitudinal cracking. While none of the treatment factors played a significant role in the initiation or propagation of NWP longitudinal cracking, the substantial precipitation that occurred in 1999 may have played a role.
- ***Transverse Cracking*:** In the FHWA-HRT-10-066 Report, a Friedman test was used to rank rehabilitation strategies in terms of transverse cracking performance (rut depth). The study found that milling with thick virgin overlays yielded the best transverse cracking performance (in terms of weighted distress or unit area under the distress performance curve) in the long-term, especially when considering the traffic and climate conditions for the Florida sites. In the FHWA-RD-01-168 Report, it was noted that in the short term, based on an analysis of variance (ANOVA), transverse cracking was most affected age of overlay, milling depth, and freeze index. From the desktop study, it was unclear what caused or propagated transverse cracking; however, environmental factors may have played a role.

- ***IRI*:** In the FHWA-HRT-10-066 Report, a Friedman test was used to rank rehabilitation strategies in terms of roughness performance (IRI). The study found that milling with thick RAP overlays yielded the best IRI performance (in terms of weighted distress or unit area under the distress performance curve) in the long-term, especially when considering the traffic and climate conditions for the Florida sites. In the FHWA-RD-01-168 Report, it was noted that in the short term, based on an analysis of variance (ANOVA), IRI was most affected by age of the overlay, condition prior to overlay, and milling depth. From the desktop study, it was found that higher initial IRI values and lower thickness led to higher deterioration rate, and that virgin overlays had a slightly lower deterioration rate than RAP.
- ***Rutting*:** In the FHWA-HRT-10-066 Report, a Friedman test was used to rank rehabilitation strategies in terms of rutting performance (rut depth). The study found that milling with thin virgin overlays yielded the best rutting performance (in terms of weighted distress or unit area under the distress performance curve) in the long-term, especially when considering the traffic and climate conditions for the Florida sites. In the FHWA-RD-01-168 Report, it was noted that in the short term, based on an analysis of variance (ANOVA), rutting was most affected by age and precipitation. Through the desktop study, because very little rutting was observed on the sites, no analysis was conducted on the initiation or propagation of rutting.

While there was general agreeance in the effect of factors that were considered in both sets of studies, the national studies also considered climate and temperature in greater detail. As expected, these factors, which were not considered in detail in this memorandum, played a role in the performance of the overlays with regards to fatigue cracking, transverse cracking, and rutting, according to the national studies.

FORENSIC EVALUATION RECOMMENDATIONS

Based on the information gathered and analysed in the above sections, further desktop evaluation of anomalies within section 12_1030 appears to be warranted. The study team will develop Data Analysis Operational Feed Back reports and submit them to LTPP staff to investigate correction of some of the issues discovered during this study. No follow-up field investigations are recommended at this time until resolution of what appears to be errors in the interpretation of LTPP measurements are corrected.

Attachment A. Photographs of SPS-5 and Control Test Sections.

Photograph 1. Picture of test section 12_0502 in 2014 (Station 0+00 looking southbound).

Photograph 2. Picture of test section 12_0503 in 2014 (Station 0+00 looking southbound).

Photograph 3. Picture of test section 12_0504 in 2014 (Station 0+00 looking southbound).

Photograph 4. Picture of test section 12_0505 in 2014 (Station 0+00 looking southbound).

Photograph 5. Picture of test section 12_0506 in 2014 (Station 0+00 looking southbound).

Photograph 6. Picture of test section 12_0507 in 2014 (Station 0+00 looking southbound).

Photograph 7. Picture of test section 12_0508 in 2014 (Station 0+00 looking southbound).

Photograph 8. Picture of test section 12_0509 in 2014 (Station 0+00 looking southbound).

Photograph 9. Picture of test section 12_0561 in 2014 (Station 0+00 looking southbound).

Photograph 10. Picture of test section 12_0562 in 2014 (Station 0+00 looking southbound).

Photograph 11. Picture of test section 12_0563 in 2014 (Station 0+00 looking southbound).

Photograph 12. Picture of test section 12_0564 in 2014 (Station 0+00 looking southbound).

Photograph 13. Picture of test section 12_0565 in 2014 (Station 0+00 looking southbound).

Photograph 14. Picture of test section 12_0566 in 2014 (Station 0+00 looking southbound).

Photograph 15. Picture of test section 12_1030 in 2014 (Station 0+00 looking southbound).